

Unified order-disorder vortex phase transition in high- T_c superconductors

Y. Radzyner, A. Shaulov, Y. Yeshurun

Department of Physics, Institute of Superconductivity, Bar-Ilan

University, Ramat-Gan, Israel

(October 30, 2001)

Abstract

The diversity of vortex melting and solid-solid transition lines measured in different high- T_c superconductors is explained, postulating a unified order-disorder phase transition driven by both thermally- and disorder-induced fluctuations. The temperature dependence of the transition line and the nature of the disordered phase (solid, liquid, or pinned liquid) are determined by the relative contributions of these fluctuations and by the pinning mechanism. By varying the pinning mechanism and the pinning strength one obtains a spectrum of monotonic and non-monotonic transition lines similar to those measured in $\text{Bi}_2\text{Sr}_2\text{CaCu}_2\text{O}_8$, $\text{YBa}_2\text{Cu}_3\text{O}_{7-\delta}$, $\text{Nd}_{1.85}\text{Ce}_{0.15}\text{CuO}_{4-\delta}$, $\text{Bi}_{1.6}\text{Pb}_{0.4}\text{Sr}_2\text{CaCu}_2\text{O}_{8+\delta}$ and $(\text{La}_{0.937}\text{Sr}_{0.063})_2\text{CuO}_4$.

Vortex matter phase transitions have been under close scrutiny in recent years. Both experimental [1–8] and theoretical [9–11] works have indicated the existence of two order-disorder phase transitions: A transition from a quasi-ordered solid phase to a liquid phase driven by thermal fluctuations, and a transition to a disordered solid phase driven by disorder-induced fluctuations. In magnetization experiments, the melting transition is signified by a jump in the reversible magnetization [1], whereas the solid-solid transition is associated with the appearance of a second magnetization peak [2,6] (‘fishtail’). A variety of experiments indicate that the melting [1] as well as the solid-solid transition [12,13] are of first order.

While melting lines measured in different samples exhibit qualitatively similar behavior, with the melting field decreasing monotonically as temperature is increased [1,3], the solid-solid transition lines measured in different samples differ markedly: A flat transition line in underdoped $\text{Bi}_2\text{Sr}_2\text{CaCu}_2\text{O}_8$ (BSSCO) [14], which terminates at intermediate temperatures; a flat transition line followed by a monotonic convex decrease toward T_c in $\text{Bi}_{1.8}\text{Pb}_{0.8}\text{Sr}_2\text{CaCu}_2\text{O}_{8+\delta}$ [15] and $\text{Nd}_{1.85}\text{Ce}_{0.15}\text{CuO}_{4-\delta}$ (NCCO) [6]; a steep concave decrease throughout the whole temperature range in $(\text{La}_{0.937}\text{Sr}_{0.063})_2\text{CuO}_4$ (LaSCO) [8] and some $\text{YBa}_2\text{Cu}_3\text{O}_{7-\delta}$ (YBCO) samples [3,16]; and a non-monotonous behavior exhibiting a peak in YBCO [3–5,13,17], BSCCO [14,18,19] and $\text{Bi}_{1.6}\text{Pb}_{0.4}\text{Sr}_2\text{CaCu}_2\text{O}_{8+\delta}$ (Pb-BSCCO) [7]. The diverse temperature dependence of the vortex solid-solid transition line is illustrated in Fig. 1 for YBCO [13], NCCO [6] and LaSCO [8] samples measured in our laboratory.

Both the melting and the solid-solid transitions may be observed in the same sample in different temperature regimes. The melting line, appearing in the high temperature region, terminates at a “critical” point [2,20] and a second line, associated with the solid-solid transition, emerges [2,6]. Recent experiments [18,21] demonstrated that the two transition lines are in fact a single line along which order is destroyed; the melting of the quasi ordered solid into a liquid at high temperatures changes its character into a solid-solid transition at low temperatures due to slower dynamics. Striking evidence for the unified nature of these two lines was recently found in vortex “shaking” experiments which show that by en-

hancing relaxation effects, the second peak anomaly is transformed into a jump in reversible magnetization [18], demonstrating that the melting and the solid-solid transition lines are different manifestations of the *same* phenomenon, i.e. a transition from an ordered phase to a disordered phase.

Motivated by the above results, and based on a recent theoretical model [9–11], we present in this paper a unified approach to the vortex order-disorder phase transition, postulating that this transition is driven by *both* thermal and disorder-induced fluctuations [11,22–25]. Our simplified analysis is capable of reproducing the markedly different behavior of the transition lines observed experimentally in different samples. A spectrum of different transition lines, with monotonic or non-monotonic behavior, is obtained by tuning the pinning strength incorporated into different pinning mechanisms.

A recent model [9–11] applies the Lindemann criterion to define a transition from an ordered state to a disordered one. Previous approaches to this model (e.g. [4–6,10]) commonly dealt with the melting and the solid-solid transitions separately, postulating that the former is driven by thermal fluctuations and the latter by disorder-induced fluctuations. Accordingly, the melting line $B_m(T)$ was determined [9,10] by a competition between the vortex lattice elastic energy and the thermal energy, whereas the solid-solid transition line $B_{ss}(T)$ was determined by a competition between the elastic energy and the pinning energy. Following this approach one encounters several difficulties. For example, one cannot explain the effect of point defects on the melting line observed experimentally [19,26]. In addition, this approach cannot explain the wide spectrum of qualitatively different solid-solid transition lines obtained in different materials, and even in different samples of the same material. In particular, contrary to the predictions of the model, which dictates a temperature independent $B_{ss}(T)$ at low temperatures, a wide spectrum of temperature dependences is observed experimentally [3–8,13–19].

The above difficulties are resolved by considering the effect of *both* thermal fluctuations and disorder-induced fluctuations in destroying the vortex lattice. The basic premise of our analysis is that an order-disorder transition occurs when the sum of the average thermal

and the disorder-induced displacements of the flux line, u_T^2 and u_{dis}^2 , respectively, exceeds a certain fraction of the vortex lattice constant a_o [11,25]. A more accurate analysis should involve the averaged total displacement of the flux line, which is not necessarily the sum of u_T^2 and u_{dis}^2 . Yet, our simplified approach yields a qualitative description, and provides important insight. Utilizing the Lindemann criterion for the destruction of order, the transition line, $B_{OD}(T)$, will obey the expression:

$$u_T^2(L_o, 0) + u_{dis}^2(L_o, 0) = c_L^2 a_o^2 \quad (1)$$

where $u_T^2(L_o, 0) = L_o kT / (2\epsilon_o \epsilon^2)$ is the transverse excursion caused by thermal agitation and $u_{dis}^2(L_o, 0) = (\xi^2/2)(L_o/L_c)^{6/5}$ is the disorder-induced fluctuation. Here, $L_o = 2\epsilon a_o$ is the characteristic length for the longitudinal fluctuations, $L_c = (\epsilon^4 \epsilon_o^2 \xi^2 / \gamma)^{1/3}$ is the size of the coherently pinned segment of the vortex [27], $\epsilon_o = (\phi_o / 4\pi\lambda)^2$ is the vortex line tension, $\epsilon = \sqrt{m_a/m_c}$ is the anisotropy ratio, c_L is the Lindemann number, $a_o = \sqrt{\phi_o/B}$ is the Abrikosov lattice constant, $\phi_o \simeq 2.07 \times 10^{-7} \text{ G} \cdot \text{cm}^2$ is the flux quantum, and γ is the pinning strength.

The transition line $B_{OD}(T)$ can also be derived [29] by considering the energy balance at the transition: The transition occurs when the sum of pinning energy and thermal energy exceeds the elastic energy barrier:

$$E_{el} = E_{pin} + kT \quad (2)$$

where $E_{el} = \epsilon \epsilon_o c_L^2 a_o$ is the elastic energy near the transition line, $E_{pin} = U_{dp} (L_o/L_c)^{1/5}$ is the pinning energy of a single vortex [9,10], and $U_{dp} = (\gamma \epsilon^2 \epsilon_o \xi^4)^{1/3}$ is the single vortex depinning energy. Both approaches Eq. (1) and (2), yield the *same* expression for $B_{OD}(T)$.

The solution of either Eq. (1) or (2) yields transition lines of different temperature dependence, depending on the pinning parameter γ and on the anisotropy ϵ . To demonstrate this variety of behaviors, we present numerical solutions for $B_{OD}(T)$, fixing ϵ so that $16\pi^2 \lambda_o^2 k / \phi_o^{5/2} \epsilon c_L^2 = 1$ [28] and varying $\Gamma_o = (2\xi_o^6 \epsilon^2 / c_L^2 k^4)^{1/5} \gamma_o^{2/5}$, i.e. controlling the pinning strength γ_o . In the calculations we use the explicit temperature dependences of the coherence length $\xi = \xi_o (1 - (T/T_c)^4)^{-1/2}$ and the penetration depth $\lambda = \lambda_o (1 - (T/T_c)^4)^{-1/2}$. We also consider two pinning mechanisms: Either “ δT_c pinning”, caused by spatial fluctua-

tions of the transition temperature T_c , or “ δl pinning”, caused by fluctuations of the charge carrier mean free path near a lattice defect [27]. In the former case the pinning parameter is $\gamma = \gamma_o^T \left(1 - (T/T_c)^4\right)^2$ and in the latter $\gamma = \gamma_o^l \left(1 - (T/T_c)^4\right)^4$ (Ref. [4]), where either γ_o^T or γ_o^l replace γ_o in the expression for Γ_o .

Fig. 2 shows the calculated order-disorder transition line $B_{OD}(T)$ (solid curve in the figure), and the irreversibility line $B_{irr}(T)$ (dashed curve) estimated by $E_{pin} = kT$, for three different values of Γ_o , assuming δT_c -pinning mechanism. For comparison we also show in Fig. 2 the ‘pure’ solid-solid transition line $B_{ss}(T)$ (dash-dotted) and ‘pure’ melting line $B_m(T)$ (dotted). $B_{ss}(T)$ is derived from $E_{el} = E_{pin}$, which neglects the thermal energy, therefore it is independent of temperature in intermediate temperature range and descends towards T_c as a result of the temperature dependences of the superconducting parameters [6]. $B_m(T)$ is a solution to $E_{el} = kT$, which neglects the pinning energy, therefore it is unaffected by changes in pinning strength. We maintain that the experimentally measured transition line - identified by either a jump in reversible magnetization or the appearance of a second peak in the irreversible magnetization - corresponds to the $B_{OD}(T)$ curve. Since the order-disorder transition is driven by *both* pinning and thermal fluctuations, $B_{OD}(T)$ will lie below both $B_m(T)$ and $B_{ss}(T)$, both of which utilize only one mechanism for the destruction of the quasi-ordered vortex lattice. The crossing point between $B_{irr}(T)$ and $B_{OD}(T)$ is the “critical point” dividing the $B_{OD}(T)$ line into two segments: The one lying above the irreversibility line will be manifested by a jump in the reversible magnetization and identified experimentally as a melting line; the other segment lying below the irreversibility line will be evinced as a second magnetization peak and identified experimentally as a solid-solid transition line.

For $\Gamma_o = 1$ (i.e. relatively small pinning parameter), the effect of pinning on the order-disorder transition is minor, therefore $B_{OD}(T)$ lies very close to the ‘pure’ melting line $B_m(T)$ and retains its concave shape (Fig. 2a). $B_{OD}(T)$ crosses the irreversibility line at extremely low temperatures, so that throughout most of the temperature range the transition will be manifested as a jump in the reversible magnetization, as measured in high purity YBCO

[30].

For $\Gamma_o = 10^6$ (relatively large pinning) the effect of temperature is small, therefore the order-disorder transition line lies near the ‘pure’ solid-solid transition line $B_{ss}(T)$ and adopts its convex shape (see Fig. 2c), as observed in NCCO [6] (see Fig. 1). In this case, the intersection of $B_{OD}(T)$ with the irreversibility line is close to T_c , so that throughout most of the temperature range the transition will be evinced as a second magnetization peak.

For $\Gamma_o = 500$ (intermediate pinning strength) the deviation of $B_{OD}(T)$ from both $B_m(T)$ and $B_{ss}(T)$ is marked (see Fig. 2b). The shape of the order-disorder transition line $B_{OD}(T)$ retains the concave shape of $B_m(T)$ but since most of the transition line lies below the irreversibility line, the transition will be manifested as a second magnetization peak. This kind of behavior of $B_{OD}(T)$ was observed in LaSCO [8] (see Fig. 1).

A non-monotonous behavior can be obtained by invoking δl -pinning mechanism, as depicted in Figure 3. In this case, $B_{ss}(T)$ is independent of temperature at intermediate temperatures, *increases* with temperature and diverges near T_c . For $\Gamma_o = 10^7$ (relatively large pinning), the incorporation of thermal fluctuations curbs this ascent, and results in a peak in $B_{OD}(T)$ as depicted in Fig. 3a. This peak may signify an inverse-melting effect [18,31] as observed experimentally in BSCCO [19], YBCO [4,31], and Pb-BSCCO [7]. An alternative explanation [4,11] to the peak in the transition line attributes this phenomenon to the depinning of the vortices by strong thermal fluctuations, which smear the pinning potential above the depinning temperature, T_{dp} . This effect was introduced into the expression for the solid-solid transition through an exponential increase of the Larkin length above the depinning temperature [4,11]. Our analysis predicts a peak in $B_{OD}(T)$ irrespective of the value of T_{dp} .

For $\Gamma_o = 10^5$ (lower pinning strength, see Fig. 3b), two phenomena are observed: The inverse-melting peak is depressed, and the critical point moves to lower temperatures. This explains the data of Khaykovich *et al.* [19] and Nishizaki *et al.* [5], showing that by repeatedly irradiating a crystal the peak in the transition line is enhanced, and the critical point shifts systematically to higher temperatures. Furthermore, a dip in the order-disorder

transition line becomes noticeable at intermediate temperatures. Such a dip was previously reported for YBCO [13,17] (see Fig. 1) and for Pb-BSCCO [7], and was attributed to Bean-Livingston barriers [32] or to masking of the fishtail onset by the field of full penetration [7]. Our analysis shows that this dip is due to the combined effect of thermally- and disorder-induced fluctuations in materials where δl -pinning is the dominant pinning mechanism. At low temperatures the elastic and pinning energies are virtually temperature independent, and $B_{ss}(T)$ is flat. Thermal fluctuations, however, become stronger as the temperature is increased causing a deviation of $B_{OD}(T)$ from $B_{ss}(T)$. The two lines (Fig. 3b) merge at low temperature, but as the temperature is increased, thermal fluctuations allow the vortices to displace and adjust to the pinning landscape and thereby induce the order-disorder transition at lower fields. This effect competes with the thermal dependence of the pinning energy, which stems from the temperature dependence of the superconducting parameters and causes $B_{ss}(T)$ to rise and diverge. At higher temperatures the latter effect wins, and the transition line $B_{OD}(T)$ increases. Further decrease of the pinning strength to $\Gamma_o = 1$ results in a monotonously decreasing order-disorder transition line (Fig. 3c).

In conclusion, we have described an order-disorder vortex phase transition driven by *both* thermal fluctuations and disorder-induced fluctuations. By varying the pinning strength a wide spectrum of transition lines is obtained, resembling those measured in various high- T_c superconductors. The intersection between the transition line and the irreversibility line defines a "critical point" which divides the transition line into two segments: One associated with the jump in the reversible magnetization and identified experimentally as a melting line, and the other associated with the 'fishtail' and identified experimentally as a solid-solid transition line. For δT_c -pinning, different pinning strengths yield monotonous transition lines similar to those obtained in clean untwinned YBCO [30], LaSCO [8] and NCCO [6]. For δl -pinning non-monotonous transition lines are obtained, with a characteristic peak as observed in YBCO [4], BSCCO [18,19] and Pb-BSCCO [7]. In addition, a decrease at low temperature, similar to that observed in YBCO [13,17] and Pb-BSCCO [7], can also be reproduced. The nature of the disordered phase may be characterized as a liquid, pinned-liquid,

or entangled solid state, depending on the relative contribution of thermal and disordered induced fluctuations. When thermal (disordered-induced) fluctuations dominate, the disordered phase exhibits liquid (disordered solid) characteristics. When both fluctuations are comparable, the disordered phase behaves as a ‘pinned-liquid’ [8].

Acknowledgments. This manuscript is part of Y.R.’s PhD thesis. Important and stimulating comments from E. Zeldov are acknowledged. Y. R. acknowledges financial support from Mifal Hapayis - Michael Landau Foundation. Y. Y. acknowledges support from the US-Israel Binational Science Foundation. A. S. acknowledges support from the Israel Science Foundation. This research was supported by The Israel Science Foundation - Center of Excellence Program, and by the Heinrich Hertz Minerva Center for High Temperature Superconductivity.

REFERENCES

- [1] E. Zeldov, D. Majer, M. Konczykowski, V. B. Geshkenbein, V. M. Vinokur, and H. Shtrikman, *Nature* **375**, 373 (1995).
- [2] B. Khaykovich, E. Zeldov, D. Majer, T. W. Li, P. H. Kes, and M. Konczykowski, *Phys. Rev. Lett.* **76**, 2555 (1996).
- [3] K. Deligiannis, P. A. J. deGroot, M. Oussena, S. Pinfold, R. Langan, R. Gagnon, and L. Taillefer, *Phys. Rev. Lett.* **79**, 2121 (1997).
- [4] D. Giller, A. Shaulov, Y. Yeshurun, and J. Giapintzakis, *Phys. Rev. B* **60**, 106 (1999).
- [5] T. Nishizaki, T. Naito, S. Okayasu, A. Iwase, and N. Kobayashi, *Phys. Rev. B* **61**, 3649 (2000).
- [6] D. Giller, A. Shaulov, R. Prozorov, Y. Abulafia, Y. Wolfus, L. Burlachkov, Y. Yeshurun, E. Zeldov, V. M. Vinokur, J. L. Peng, and R. L. Greene, *Phys. Rev. Lett.* **79**, 2542 (1997).
- [7] M. Baziljevich, D. Giller, M. McElfresh, Y. Abulafia, Y. Radzyner, J. Schneck, T. H. Johansen, and Y. Yeshurun, *Phys. Rev. B* **62**, 4058 (2000).
- [8] Y. Radzyner, A. Shaulov, Y. Yeshurun, I. Felner, J. Shimoyama, and K. Kishio, *Phys. Rev. B* (in print).
- [9] D. Ertas and D. R. Nelson, *Physica C* **272**, 79 (1996).
- [10] V. Vinokur, B. Khaykovich, E. Zeldov, M. Konczykowski, R. A. Doyle, and P. H. Kes, *Physica C* **295**, 209 (1998).
- [11] T. Giamarchi and P. LeDoussal, *Phys. Rev. B* **55**, 6577 (1997).
- [12] S. B. Roy and P. Chaddah, *Physica C* **279**, 70 (1997).
- [13] Y. Radzyner, S. B. Roy, D. Giller, Y. Wolfus, A. Shaulov, P. Chaddah, and Y. Yeshurun,

- Phys. Rev. B **61**, 14362 (2000)..
- [14] Y. Yamaguchi, G. Rajaram, N. Shirakawa, A. Mumtaz, H. Obara, T. Nakagawa, and H. Bando, Phys. Rev. B **63**, 014504 (2001).
- [15] Y. P. Sun, Y. Y. Hsu, B. N. Lin, H. M. Luo, and H. C. Ku, Phys. Rev. B **61**, 11301 (2000).
- [16] M. Pissas, E. Moraitakis, G. Kallias, and A. Bondarenko, Phys. Rev. B **62**, 1446 (2000).
- [17] H. Kupfer, T. Wolf, R. Meier-Hirmer, and A. A. Zhukov, Physica C **332**, 80 (2000).
- [18] N. Avraham, B. Khaykovich, Y. Myasoedov, M. Rappaport, H. Shtrikman, D. E. Feldman, T. Tamegai, P. H. Kes, M. Li, M. Konczykowski, K. van der Beek, and E. Zeldov, Nature **411**, 451 (2001).
- [19] B. Khaykovich, M. Konczykowski, E. Zeldov, R. A. Doyle, D. Majer, P. H. Kes, and T. W. Li, Phys. Rev. B **56**, R517 (1997).
- [20] H. Safar, P. L. Gammel, D. A. Huse, D. J. Bishop, W. C. Lee, J. Giapintzakis, and D. M. Ginsberg, Phys. Rev. Lett. **70**, 3800 (1993).
- [21] C. J. van der Beek, S. Colson, M. V. Indenbom, and M. Konczykowski, Phys. Rev. Lett. **84**, 4196 (2000).
- [22] Y. Y. Goldschmidt, Phys. Rev. B **56**, 2800 (1997).
- [23] V. Vinokur, B. Khaykovich, and E. Zeldov, unpublished and private communication.
- [24] J. Kierfeld and V. Vinokur, Phys. Rev. B **61**, R14928 (2000).
- [25] G. P. Mikitik and E. H. Brandt, Phys. Rev. B **64**, 184514 (2001) .
- [26] A. Soibel, E. Zeldov, M. Rappaport, Y. Myasoedov, T. Tamegai, S. Ooi, M. Konczykowski, and V. B. Geshkenbein, Nature **406**, 282 (2000).
- [27] G. Blatter, M. V. Feigelman, V. B. Geshkenbein, A. I. Larkin, and V. M. Vinokur, Rev.

Mod. Phys. **66**, 1125 (1994).

[28] Increasing or decreasing the anisotropy results in the same variety of lines depicted in Fig. 2, but which correspond now to different values of the pinning strength.

[29] Y. Radzyner *et. al*, preprint.

[30] A. Junod, M. Roulin, J. Y. Genoud, B. Revaz, A. Erb, and E. Walker, Physica C **275**, 245 (1997).

[31] S. B. Roy, Y. Radzyner, D. Giller, Y. Wolfus, A. Shaulov, P. Chaddah, and Y. Yeshurun, cond-mat/0107100 (2001).

[32] M. C. de Andrade, N. R. Dilley, F. Ruess, and M. B. Maple, Phys. Rev. B **57**, R708 (1998).

Figure Captions

Figure 1: Vortex solid-solid transition lines measured in YBCO (triangles), NCCO (squares) and LaSCO (circles), exhibit different qualitative behavior. Transition field is normalized to its value at lowest temperature 20.5 kOe, 260 G, 11.8 kOe respectively; temperature is normalized by $T_c = 93, 26, 32$ K respectively.

Figure 2: Calculated order-disorder transition line, $B_{OD}(T)$ (solid curve), irreversibility line $B_{irr}(T)$ (dashed), ‘pure’ melting line $B_m(T)$ (dotted) and ‘pure’ solid-solid transition line $B_{ss}(T)$ (dashed-dotted), for three different values of pinning strength assuming δT_c -pinning mechanism. Stars mark critical points.

Figure 3: Same as Fig. 2 assuming δl -pinning mechanism.

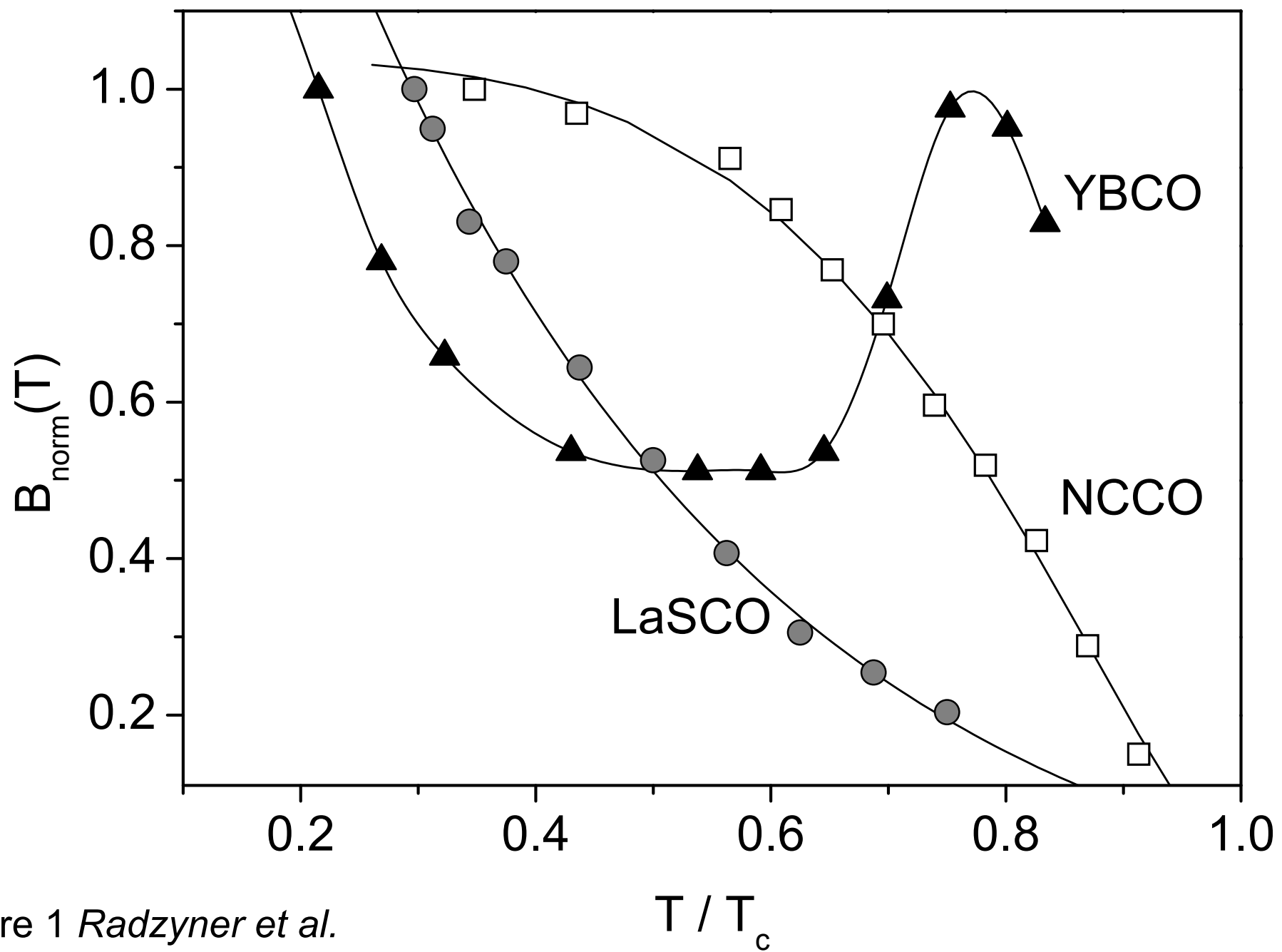


Figure 1 *Radzyner et al.*

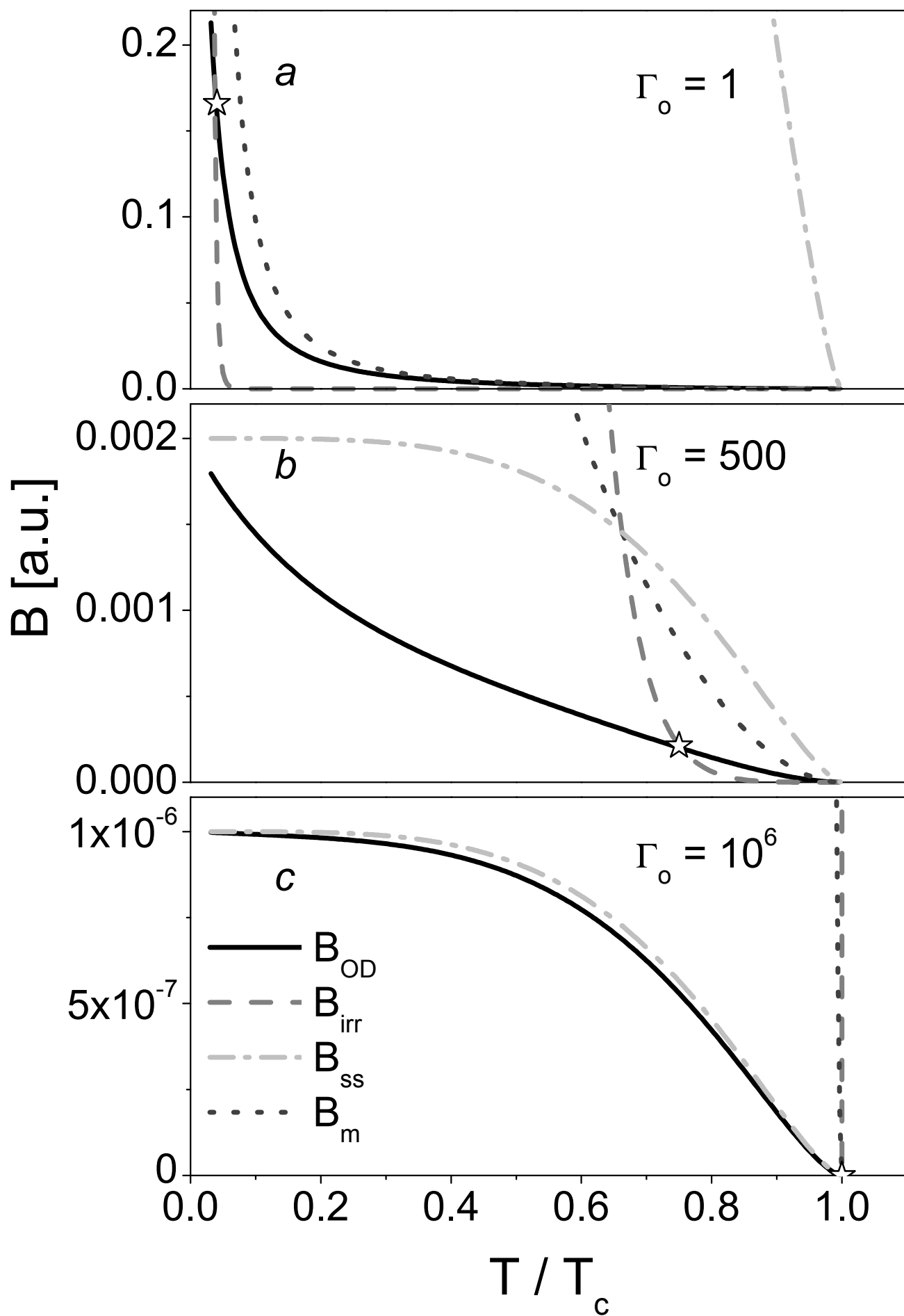


Fig. 2 Radzyner et al.

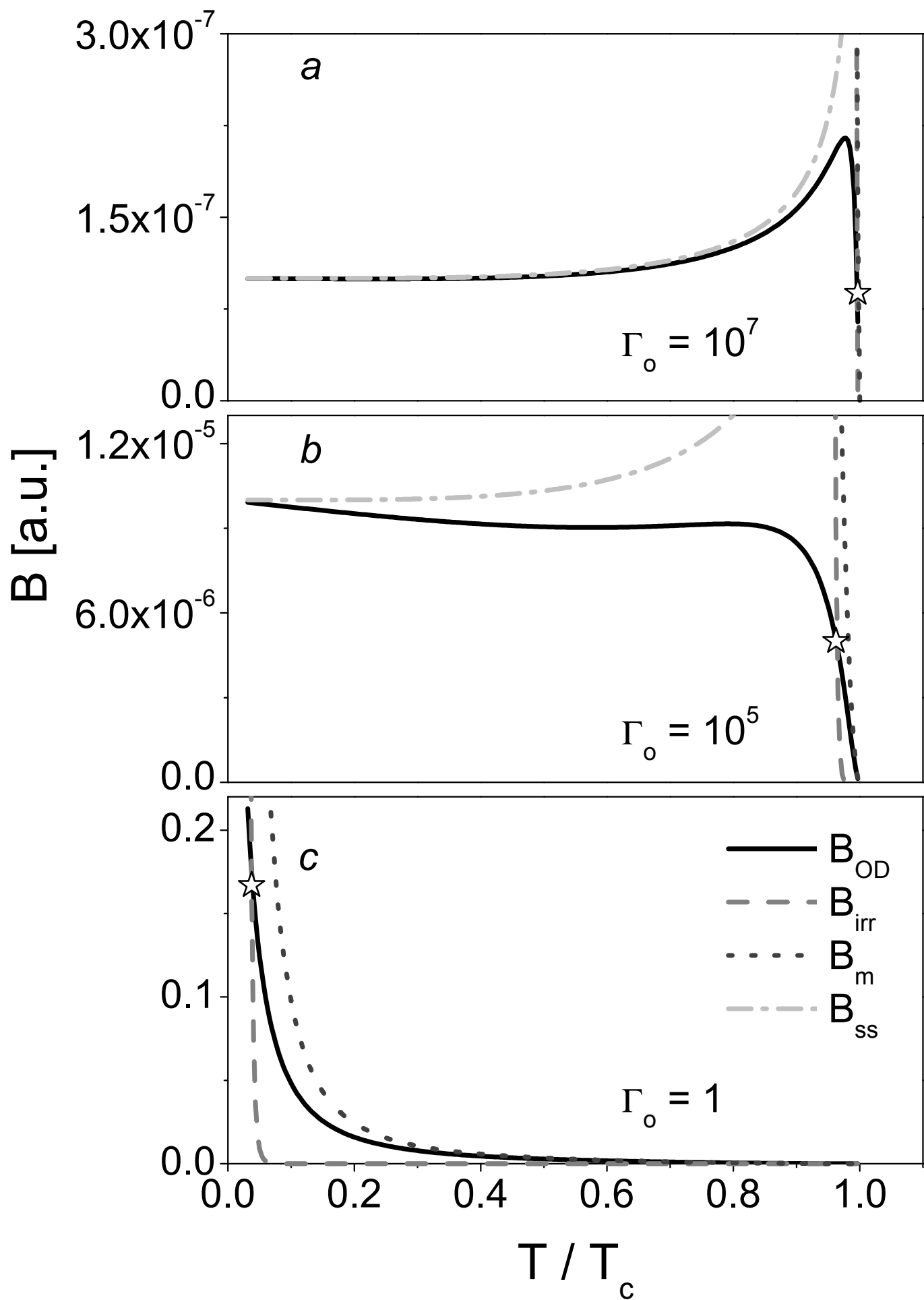


Fig. 3 Radzyner et al.